Supplementary data for

Phase transformation as the mechanism of mechanical deformation of vertically aligned carbon nanotube arrays: Insights from mesoscopic modeling

Bernard K. Wittmaack,[a] Alexey N. Volkov,[b] and Leonid V. Zhigilei [a]

[a] Department of Materials Science and Engineering, University of Virginia, 395 McCormick Road, Charlottesville, Virginia 22904-4745, USA

[b] Department of Mechanical Engineering, University of Alabama, Hardaway Hall, 7th Avenue, Tuscaloosa, Alabama 35487, USA

Contents

1. The effect of fracture on the deformation behavior of VACNT forests

The simulations reported in the present paper are performed with a model that accounts for the possibility of both axial and bending fracture of individual CNTs. For (10,10) single-walled carbon nanotubes (SWCNTs), the axial fracture is set to occur at a local strain of 0.279 [1], and the bending fracture occurs at a local bending angle of 120° [2]. In the course of the uniaxial compression up to the strain of 0.9, however, only the bending fracture of some of the nanotubes is observed at the late stage of the VACNT forest compression. In particular, approximately 8% of the 2,500 CNTs in the sample FA fracture due to bending by the time the compressive strain reached the level of 0.8. The number of CNT fracture events is 3% for sample FB, 9% for sample FC, and 17% for sample FD at 0.8 strain. The number of fractured CNTs at 0.8 strain increases from sample FB to sample FD by more than a factor of 5. The reason is that the average inclination of CNTs with respect to the vertical direction is substantially higher in sample FD than in sample FB, resulting in higher connectivity between CNT bundles. The individual CNTs and thin bundles that connect the larger bundles in sample FD are more prone to fracture during compression.

In order to check the effect of the bending fracture on the stress – strain relationship and the mechanisms of the deformation, the simulation for sample FD, where the fracture is most extensive, is repeated with a force field where the possibility of the fracture is switched off. Although almost a fifth of CNTs undergo fracture in this sample during the compression to 0.8 strain in one simulation and the possibility of fracture is eliminated in another, the difference in the stress response, CNT-CNT interaction energy, and bending energy in the two simulations is small (see Fig. S1). Even at higher strains, the evolution in stress, bending and CNT-CNT interaction energies is qualitatively similar and the overall picture of deformation (*i.e.*, the formation of the localized densified phase) is unaltered when the nanotube fracturing is neglected (Fig. S1b,c,d). Thus, we can conclude that the general deformation behavior, the CNT-CNT interaction energies, and the stress on the indenter are not significantly affected by the criteria assumed for the onset of fracture of the individual nanotubes.

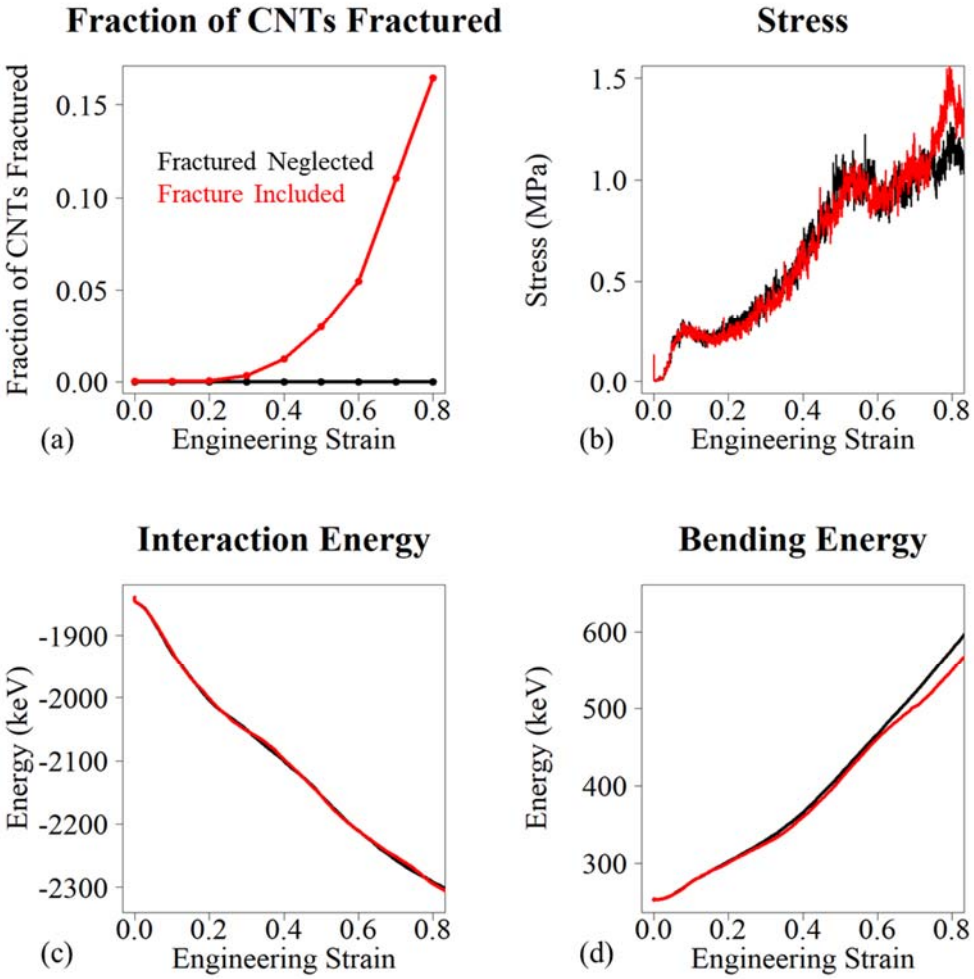

Fig. S1: Fraction of fractured CNTs (a), stress (b), CNT-CNT interaction energy (c), and bending energy (d) plotted as a function of engineering strain for VACNT sample FD. The results are shown for simulations where the possibility of CNT fracture is included (black lines) and neglected (red lines).

2. Images of the initial structure of computational samples

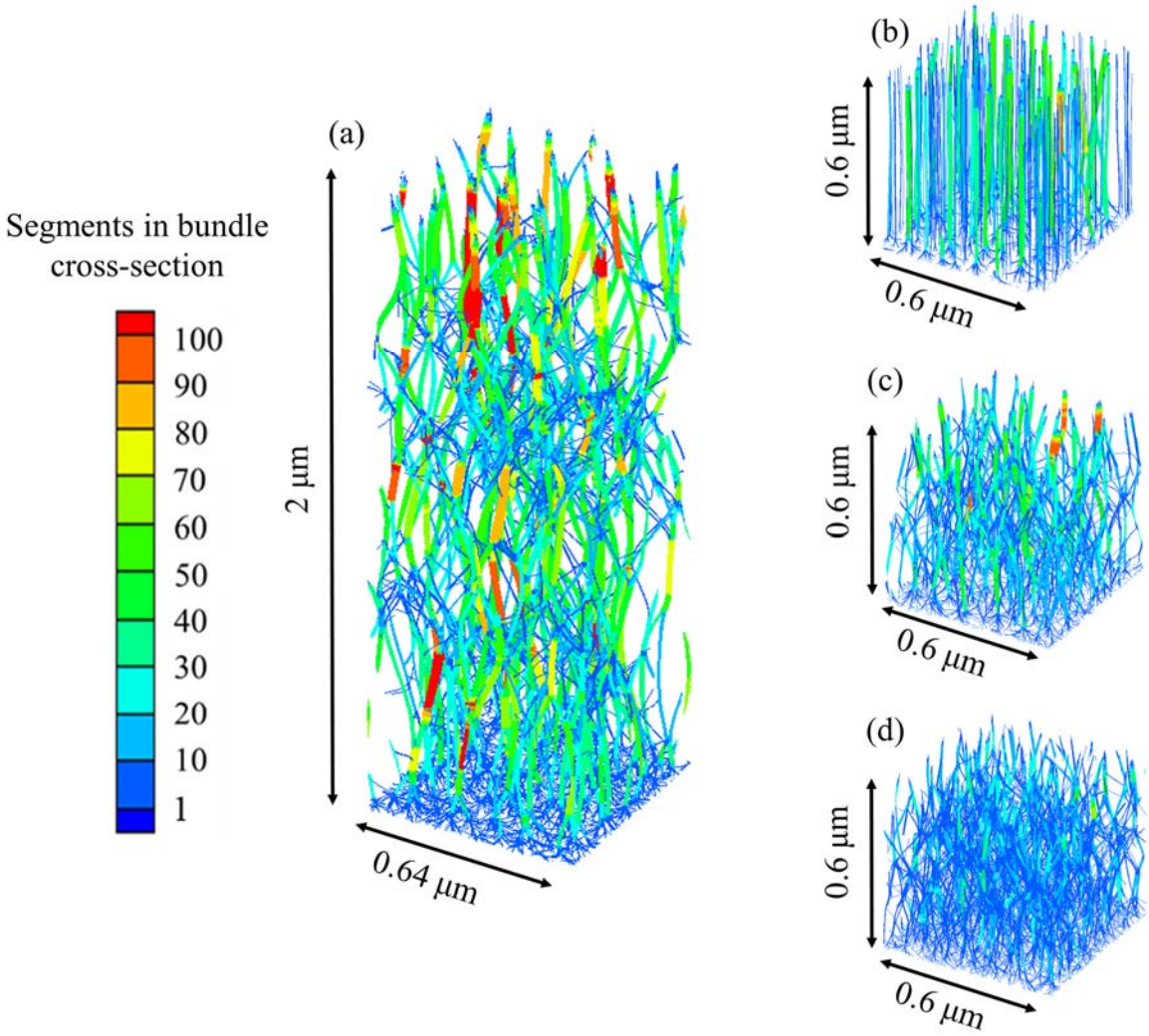

Fig. S2: Side views of computational VACNT samples composed of 2-μm-long CNTs, FA (a) and 0.6-μm-long CNTs, FB, FC, and FD (b-d) generated in mesoscopic simulations. The CNT segments are colored by the local bundle thickness (number of segments in a bundle cross section).

3. Evidence for the quasi-static nature of the compressive deformation (absence of the shock wave generation).

The experimental observation of the formation of densified regions under conditions of rapid deformation of VACNT forests have been attributed to the formation and propagation of a shock wave with a sharp front separating the low- and high-density regions of the compressed sample [3]. In order to check this hypothesis, an additional simulation was performed for sample FA, where the compression was stopped at 0.4 strain and the evolution of the system was followed for additional 16 ns with no additional deformation (the movement of the indenter was stopped at 16 ns, when the engineering strain reached the level of 0.4). As can be seen from Figs. S3 and S4, the inter-tube interaction and bending energies (Fig. S3) stay at almost constant levels after the compression is halted, and the interface separating the dense horizontally-oriented phase from the rarified vertically-oriented one (Fig. S4) ceases to advance with the absence of further deformation. These observations are inconsistent with the notion of densification driven by the shock wave propagation, as the forest structure would be expected to continue to evolve after the indenter is stopped in this case. Thus, the formation of the densified region in the simulation cannot be attributed to the shock wave formation.

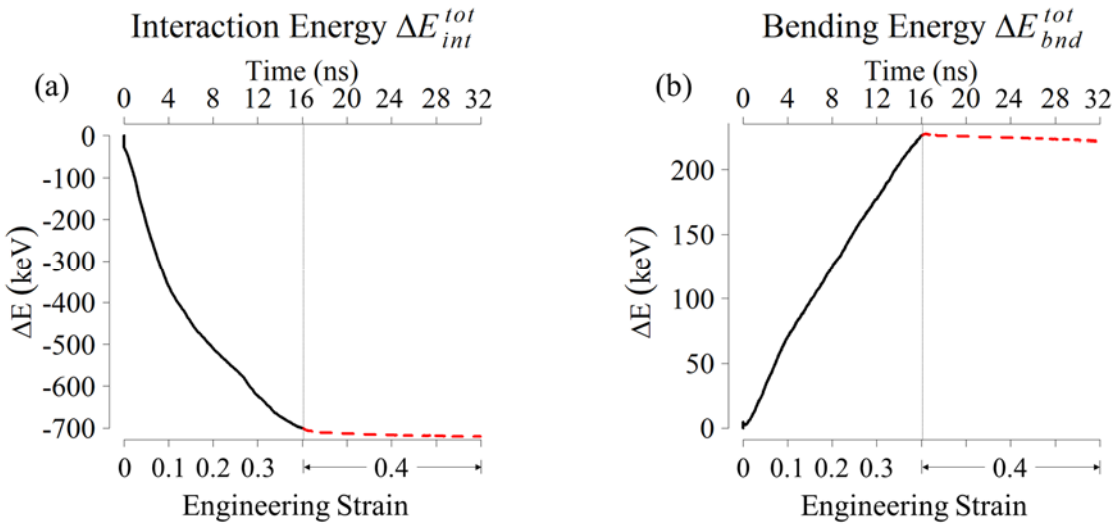

Fig. S3: The total change in the inter-tube interaction energy ΔE_{int}^{tot} (a) and bending energy ΔE_{bnd}^{tot} (b) during the compressive deformation of sample FA up to the maximum engineering strain of 0.4 (black solid lines), and a subsequent evolution of the forest without further compression for additional 16 ns (red dashed lines).

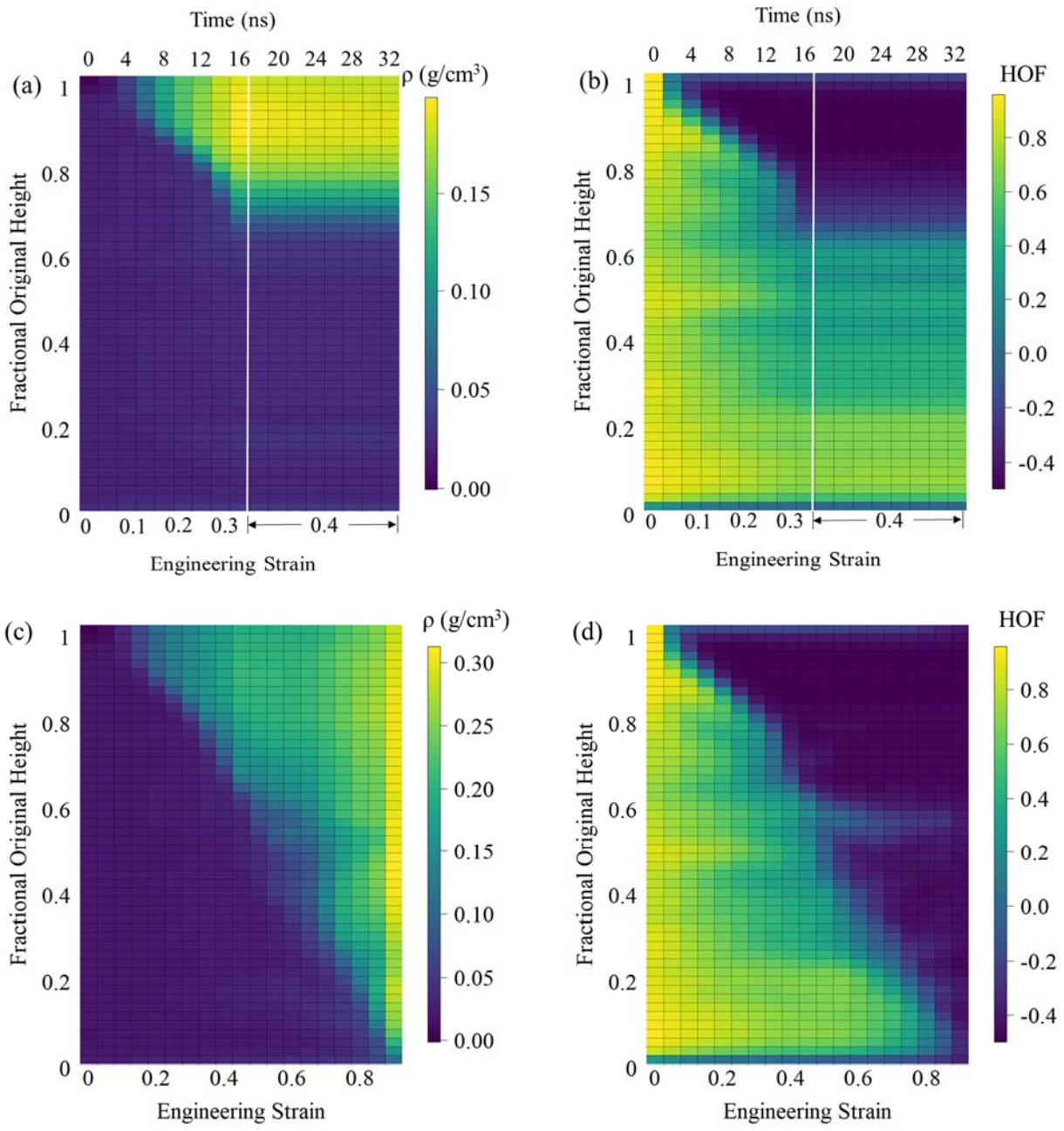

Fig. S4: Contour plots of the mass density ρ (a) and local HOF (b) calculated for VACNT sample FA that is first compressed to 0.4 strain and then allowed to evolve without further deformation (fixed position of the indenter) for additional 16 ns. For comparison, the contour plots of density and HOF are reproduced from Fig. 3 for the same sample continuously compressed down to 0.9 strain in (c) and (d). The vertical white lines in (a,b) mark the time when the compressive deformation is stopped. In addition to the engineering strain, the time from the start of the deformation is shown on the upper *x* axes for (a) and (b).

4. Snapshots of sample FA with five representative CNTs highlighted.

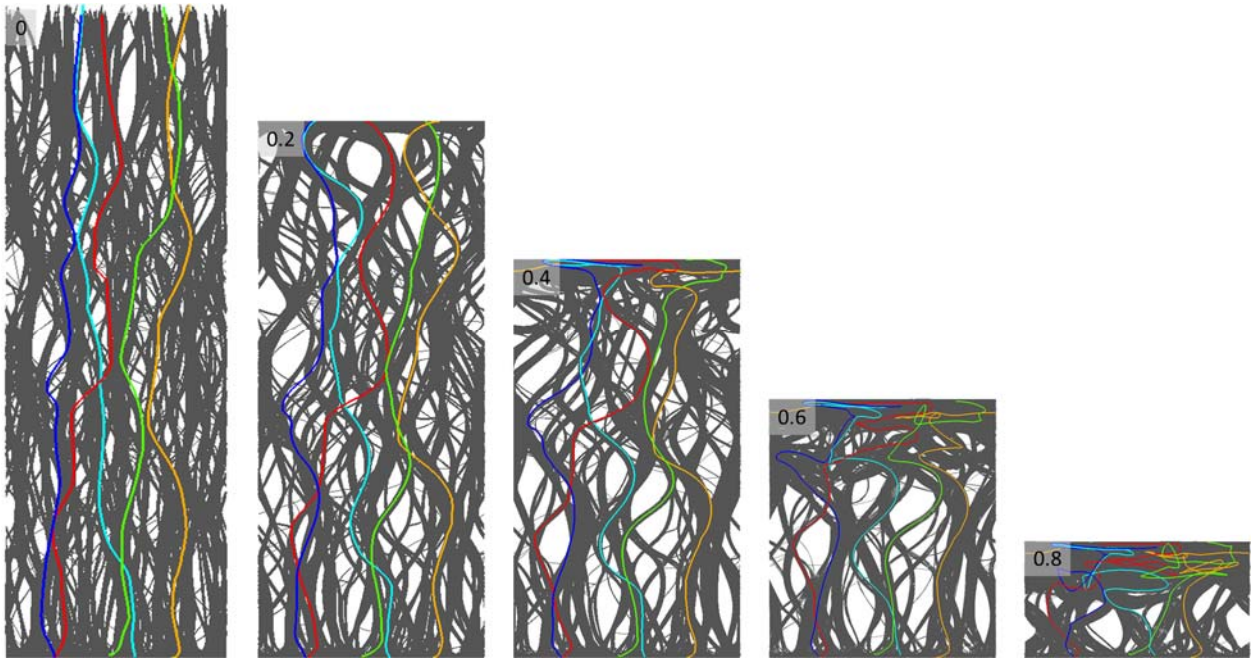

Fig. S5: Side-view snapshots of sample FA undergoing compressive deformation shown with 0.2 strain increments. Five representative CNTs are overlaid on the images and are shown in different colors to highlight the nanotube shape evolution during the deformation.

References

[1] K.M. Liew, X.Q. He, C.H. Wong, On the study of elastic and plastic properties of multi-walled carbon nanotubes under axial tension using molecular dynamics simulation, Acta Mater. 52(9) (2004) 2521-2527.

[2] S. Iijima, C. Brabec, A. Maiti, J. Bernholc, Structural flexibility of carbon nanotubes, J. Chem. Phys. 104(5) (1996) 2089-2092.

[3] R. Thevamaran, E.R. Meshot, C. Daraio, Shock formation and rate effects in impacted carbon nanotube foams, Carbon 84 (2015) 390-398.